Bubble motion and jetting at sonotrodes

T. Nowak[1], R. Mettin[2], W. Lauterborn
Drittes Physikalisches Institut, Universität Göttingen, Friedrich-Hund-Platz 1, 37077 Göttingen, Germany
Email: [1] *T.Nowak@physik3.gwdg.de,* [2] *R.Mettin@physik3.gwdg.de*

Introduction

Although acoustic cavitation [1, 2] is used in many applications, some phenomena still are hardly understood, for example, the interaction of bubbles in complex bubble structures, or the effect of interfaces nearby on collapsing bubbles. Sonotrodes or Mason-horns [3] are commonly used to generate acoustic cavitation, without having an adequate description of the processes taking place at the tip yet. While the gross structures are well known, the behaviour of single bubbles in such cavitation fields is barely investigated. Some recent results have been given by Moussatov *et al.* [4], Mettin [5] and Yasui *et al.* [6]. Here we aim at a more detailed investigation of single bubble collapses and jumps close to a sonotrode tip, as already observed in earlier work by our group [7, 8]. Furthermore, we are interested in the frequency dependence of the bubble behaviour at specific transducer types to discriminate between "frequency" and "transducer" effects. In this line, sonotrodes for different frequencies and with scaling of the emitter size were developed. This paper describes the motion and oscillation of bubbles in water near the tip of sonotrodes at 20 kHz and 60 kHz, observed by high speed imaging, and compares the results with simulations.

Experimental results

Long time observations

To observe bubbles on longer time scales, a high-speed recording (Photron APX-RS) with 10000 fps was taken for the 20 kHz sonotrode (tip diameter 10 mm). A pseudo streak image has been produced by cutting a small stripe out of every movie frame (see Fig. 1). On this time scale the visible bubbles move clearly towards the sonotrode. The bubbles are getting faster the closer they come, growing in size on their way to the sonotrode tip, as can be resolved from Fig. 1.

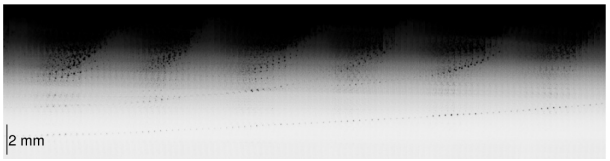

Figure 1: Bubble motion on a longer time scale (20 kHz sonotrode tip visible in the upper part of the stripes). Consecutive frame stripes taken from a movie recorded with 10000 fps and 2 µs exposure, time from left to right.

The paths of some bubbles apparent in this movie were measured and plotted for a clear demonstration in Fig. 2. Comparing different bubbles a relationship between their speed and their (maximum) size is found: the bigger the bubbles expand, the faster they are.

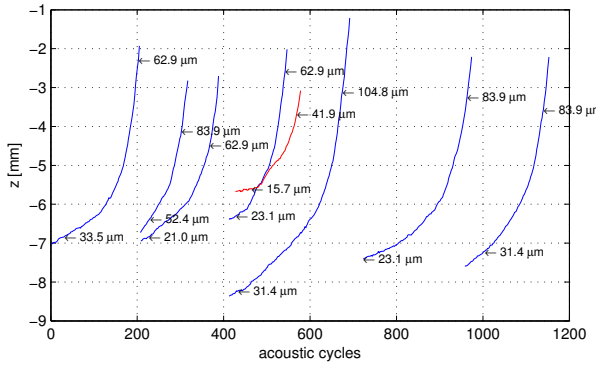

Figure 2: Bubble motion below the tip of the 20 kHz sonotrode. Bubble paths taken from the same movie as Fig. 1 but for a longer period of time. The arrows mark the observed maximum radii at the selected start and stop times.

Selected start and end radii are shown in Fig. 2 marked by arrows. One observes that the radii are getting larger when approaching the sonotrode tip. In some other movies, not shown here, smaller bubbles become visible which move away from the sonotrode (compare [8]), probably by bulk liquid motion due to acoustic streaming.

Corresponding recordings have been done at a 60 kHz sonotrode (tip diameter 1 mm). The bubble analysed in Fig. 3 shows a very similar behavior to the 20 kHz case. Here also the radius of the bubble grows the more the closer it comes to the sonotrode tip. Note that the absolute acoustic pressure is unknown in the recordings, and that therefore the distances of the bubbles from the sonotrode tips at 20 and 60 kHz cannot be directly compared.

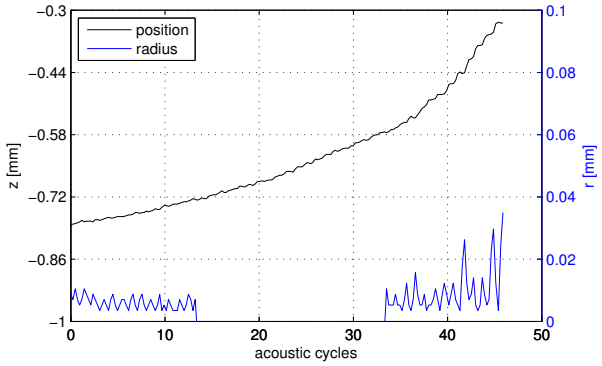

Figure 3: Bubble motion below the tip of a 60 kHz sonotrode. Bubble path taken from a movie recorded with 250000 fps and 1 µs exposure. The radial oscillations in the middle (which are not printed) remain very similar to those in the beginning.

High speed observations

To analyse single bubbles more closely, a rather confined field of view has been selected with the high speed camera under the 20 kHz sonotrode, marked in Fig. 4 by a white rectangle. From the magnified recordings from this area in Fig. 5, one can see a clear jumping in the moment of bigger bubbles' collapse. In the expanding phase, they move away from the sonotrode, but when collapsing, they jump towards it. This behaviour is clearly resolved in the figure, and also the repelling of small bubbles is visible here. Additionally it can be seen in Figs. 5 and 6 that forward jetting and shape perturbations prevent the bubble from reexpanding fully in the next period. This behaviour has partly been predicted theoretically by Szeri *et al.* [9, 10]. In the form observed here, it is a possible reason for period two (or higher) bubble oscillations, and consequently can constitute a source of subharmonic sound radiation in the acoustic emission spectra.

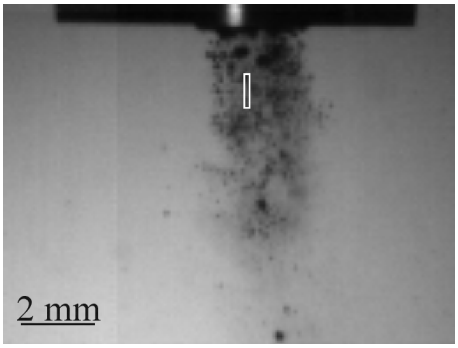

Figure 4: The bubble field under the sonotrode (20 kHz sonotrode tip visible in the upper part of the picture). The white frame marks the position of the field of view of the pseudo streak image of Fig. 5.

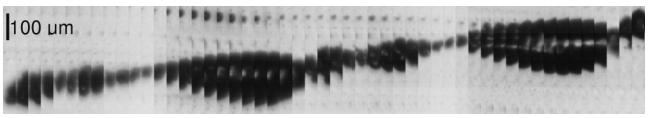

Figure 5: Pseudo streak image of a big and a small bubble beneath the tip of a 20 kHz sonotrode taken from a movie with a field of view shown in Fig. 4. Recorded with 250000 fps and 1 µs exposure time.

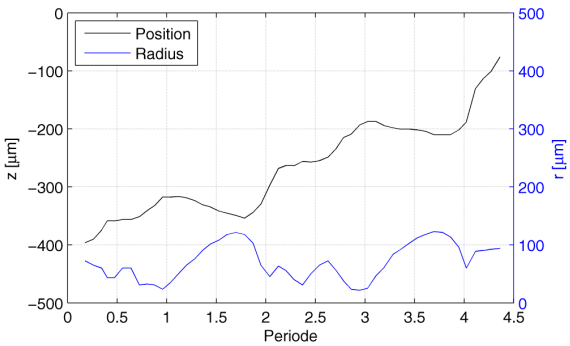

Figure 6: Evaluation of position and radius vs. driving period for the big bubble shown in Fig. 5.

At the 60 kHz sonotrode a similar recording shows the jumping behavior of bigger bubbles as well. Figure 7 gives an overview of the bubble field and the magnified area below the sonotrode tip (white rectangle). A pseudo streak example is shown in Fig. 8. Again, smaller bubbles drift away (downwards) from the tip, and larger bubbles jump upwards during collapse. Furthermore, as in the 20 kHz case, jetting and shape perturbations are visible, and incomplete reexpansions are apparent. Of course, the limited camera speed and the smaller scale constrain a more detailed monitoring at the higher acoustic frequency.

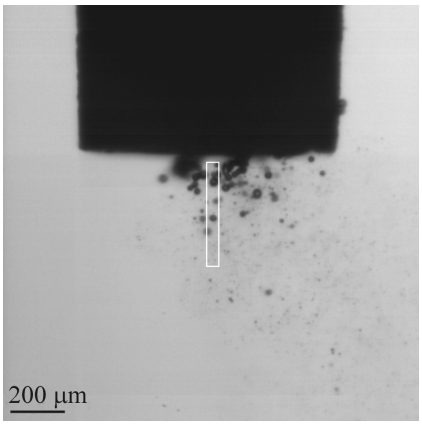

Figure 7: The bubble field under the 60 kHz sonotrode (tip visible in the upper part of the picture). The white frame marks the position of the field of view in the next figure.

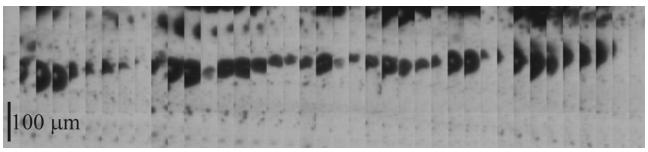

Figure 8: Pseudo streak image from a recording with the magnified field of view shown in figure 7. Recorded with 250000 fps and 1 µs exposure time.

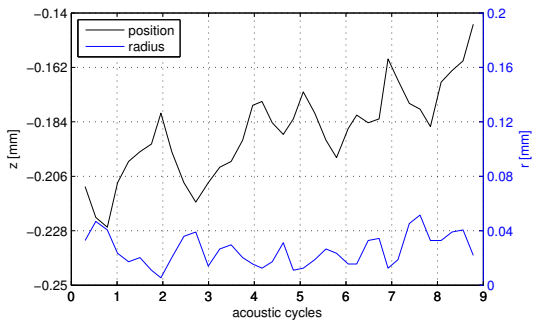

Figure 9: Evaluation of position and radius vs. acoustic driving periods for the large bubble shown in figure 8. The sonotrode tip is placed at $z = 0$.

Theoretical results

The bubble behaviour under the sonotrode tip has been simulated by a spherical single bubble model that includes volume oscillations together with translational dynamics. While the oscillation is captured by a standard Keller-Miksis model [11], the translation is calculated by

the following equation of motion:

$$\frac{2\pi}{3}\rho\frac{\mathrm{d}}{\mathrm{d}t}\left(R\left(t\right)^3\left(U_{\mathrm{A}}\left(t\right)-\dot{X}\left(t\right)\right)\right)$$
$$=\frac{4\pi}{3}R\left(t\right)^3\nabla P_{\mathrm{A}}\left(X\left(t\right),t\right)-12\pi\mu R\left(t\right)\left(U_{\mathrm{a}}\left(t\right)-\dot{X}\left(t\right)\right)\ ,$$

where R is the bubble radius, P_A the external pressure, $U_{\mathrm{a}}\left(t\right) = \dot{X}\left(t\right) + U\left(t\right)$ is the total bubble velocity according to the difference between relative speed of the liquid to the bubble, $U\left(t\right)$, and the bubble velocity, $\dot{X}\left(t\right)$. The position of the bubble centre is indicated by $X\left(t\right)$, ρ and μ are liquid density and viscosity.

The external sound field is assumed to follow the formula of a piston source [12] with an additional component from a bigger bubble being attached directly at the sonotrode tip (compare Fig. 4 where a bigger attached gas volume is visible).

The results for two bubbles of different size are shown in Fig. 10. The simulations are done without inclusion of acoustic streaming, which would point away from the tip. The small bubble (red) is only weakly oscillating and is driven very weakly by Bjerknes forces towards the sonotrode (upwards). This motion would not compensate the streaming, which would result in a net downward drift. In contrast, the bigger bubble (blue) with strong pulsations shows a distinct (upward) jump during collapse due to conservation of Kelvin impulse (or, stated differently, the dramatic shrinkage of virtual mass during collapse), and this motion overcomes any streaming by far. Furthermore, the jumps get larger the closer the bubble approaches the tip. Of course, the disturbance of spherical shape is not captured by the model, which should lead to an overestimation of the jump distance. Nevertheless, main features of the experimental observation can be reproduced well by this simple simulation.

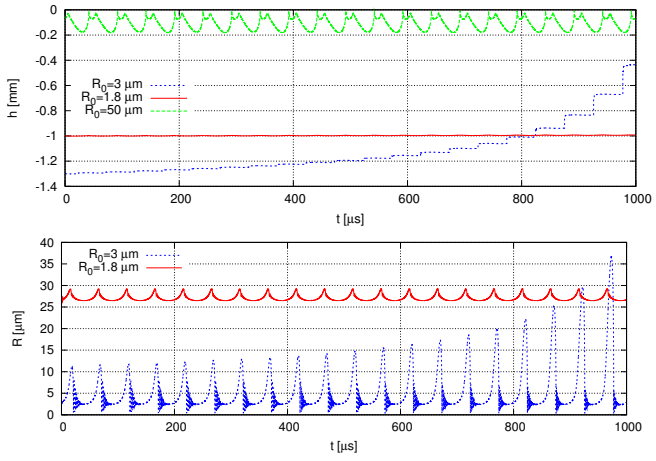

Figure 10: Simulation of oscillation and position of three bubbles in the sound field below a 20 kHz sonotrode. The green curve in the top graph depicts the radius of a big bubble attached to the sonotrode tip (radius vs. time t, inverted curve, sonotrode tip at $h = 0$). The radial oscillations vs. time of a "small" and a "bigger" bubble are given by the red and blue curves in the bottom graph. Their positions are shown by red and blue lines, respectively, in the top graph.

Conclusions

We presented some long time and acoustic period resolved observations of single bubbles near sonotrode tips operated at 20 kHz and 60 kHz. The results demonstrate jumping, jetting, splitting and sometimes repelling of these bubbles. The jumping behaviour can be captured by a simple oscillation-translation model of a single spherical bubble in a piston source pressure field. In some cases the splitting of smaller bubbles and very strong surface perturbations lead to period two (or higher) oscillations which has been observed both at 20 kHz and 60 kHz. This can be interpreted as another source of subharmonic acoustic emissions by cavitating liquids. For the visualisation of even more details, already at 60 kHz the camera speed is the limiting factor. Faster cameras might show a similar behaviour even at higher acoustic frequencies and thus prove the universality of jumping and jetting of bubbles at this type of ultrasound emitter.

References

[1] F.R. Young, *Cavitation*, McGraw-Hill 1989.

[2] T.G. Leighton, *The Acoustic Bubble*, Academic Press 1994.

[3] W. P. Mason, R. Wick, "A Barium Titanate Transducer Capable of Large Motion at an Ultrasonic Frequency", J. Acoust. Soc. Am. **23**(2), 209-214 (1951).

[4] A. Moussatov, R. Mettin, C. Granger, T. Tervo, B. Dubus, W. Lauterborn, "Evolution of acoustic cavitation structures near larger emitting surface", in: *Proceedings of the World Congress on Ultrasonics, Sept. 7-10, 2003*, Paris (France), pp. 955-958.

[5] R. Mettin, "Bubble structures in acoustic cavitation", in: A. A. Doinikov (ed.): *Bubble and Particle Dynamics in Acoustic Fields: Modern Trends and Applications*, Research Signpost, Kerala (India) 2005, pp. 1-36.

[6] K. Yasui, Y. Iida, T. Tuziuti, T. Kozuka, A. Towata, "Strongly interacting bubbles under an ultrasonic horn," Phys. Rev. E **77**, 016609 (2008).

[7] R. Mettin, "From a single bubble to bubble structures in acoustic cavitation", in: T. Kurz, U. Parlitz, U. Kaatze (eds.): *Oscillations, Waves and Interactions*, Universitätsverlag Göttingen, Göttingen, 2007, pp. 171-198.

[8] R. Mettin, T. Nowak, "Experimentelle Beobachtung der sprunghaften Blasenbewegung in Kavitationsfeldern", in: U. Jekosch, R. Hoffmann (Hrsg.): Fortschritte der Akustik - DAGA 2008 Dresden, Deutsche Gesellschaft für Akustik e.V. (DEGA), Berlin, 2008, pp. 479-480.

[9] A. J. Reddy, A. J. Szeri, "Shape stability of unsteadily translating bubbles," Phys. Fluids **14**, 2216-2224 (2002)).

[10] M. L. Calvisi, O. Lindau, J. R. Blake, A. J. Szeri, "Shape stability and violent collapse of microbubbles in acoustic traveling waves," Phys. Fluids **19**, 047101 (2007).

[11] U. Parlitz, V. Englisch, C. Scheffczyk, W. Lauterborn, "Bifurcation structure of bubble oscillators," J. Acoust. Soc. Am. **88**, 1061 (1990).

[12] H. Kuttruff, *Physik und Technik des Ultraschalls*, Hirzel Verlag, Stuttgart 1988.